Sympathetic cooling in a mixture of diamagnetic and paramagnetic atoms

S. Tassy, N. Nemitz, F. Baumer, C. Höhl, A. Batär and A. Görlitz

Institut für Experimentalphysik, Heinrich-Heine-Universität Düsseldorf, Universitätsstraße 1, 40225 Düsseldorf, Germany

E-mail: axel.goerlitz@uni-duesseldorf.de

Abstract. We have experimentally realized a hybrid trap for ultracold paramagnetic rubidium and diamagnetic ytterbium atoms by combining a bichromatic optical dipole trap for ytterbium with a Ioffe-Pritchard-type magnetic trap for rubidium. In this hybrid trap, we have investigated sympathetic cooling for five different ytterbium isotopes through elastic collisions with rubidium. A strong dependence of the thermalization rate on the mass of the specific ytterbium isotope was observed.

PACS numbers: 34.50.Cx, 37.10.De, 37.10.Gh

Keywords: ultracold collisions, sympathetic cooling, atom trapping, ytterbium

1. Introduction

The realization of mixtures of ultracold atomic gases in conservative atom traps has opened the way for the study of new fundamental aspects in dilute quantum degenerate systems. Various combinations of alkali atoms have successfully been trapped in conservative traps and recently even simultaneous trapping of three different alkali species has been reported [1]. Among the experimental achievements in these systems are the realization of two-species Bose-Einstein condensates [2], quantum degenerate Bose-Fermi [3, 4, 5] and Fermi-Fermi [1, 6] mixtures and the realization of interspecies Feshbach resonances [7, 8, 9, 10, 11, 12]. One of the most intriguing aspects of the physics of ultracold mixtures is the preparation of a trapped sample of ultracold heteronuclear molecules in the rovibrational ground state, which offers fascinating possibilities to study ultracold dipolar gases [13], explore new systems for quantum information [14, 15] or test fundamental physics [16, 17]. In bialkali systems several groups have observed ultracold molecules in the rovibrational ground state in the last few years [18, 19, 20, 21] and recently, these studies led to observations of quantum stated controlled chemical reactions [22, 23].

So far, experimental studies of ultracold mixtures in conservative traps were limited to bialkali systems. Only recently, several groups have begun to investigate mixtures of alkali atoms with ytterbium (Yb) and first experimental results of magneto-optical trapping [24, 25] and photoassociation [24] have been obtained. Conservative trapping of such mixtures is complicated by the fact that the ground state of Yb is diamagnetic while the ground state of alkali atoms is paramagnetic. Hence, trapping of both species in a common magnetic trapping potential is not possible, in contrast to alkali mixtures where magnetic traps are typically used for evaporative cooling of the mixture. The alternative approach of optical trapping of the mixture is also not straightforward as the polarizability of Yb (and alkaline earth atoms) is significantly smaller than that of alkali atoms for most wavelengths that are typically used for optical trapping. The resulting different trap depths are a severe limitation for many experimental studies.

In this work, we report on an experimental solution for simultaneous trapping and cooling of alkali and diamagnetic atoms such as Yb in a hybrid trap. In our experimental setup, rubidium (Rb) and Yb are held in two separate but spatially overlapping traps. The trapping scheme uses a clover leaf magnetic trap (MT) [26] for Rb and a bichromatic optical dipole trap for Yb and thus offers the flexibility to manipulate the two species independently. As a consequence, the interspecies interactions can be turned on or off by controlling the spatial overlap of the two atomic clouds.

The BIODT for Yb is created by two superimposed laser beams at 532 nm and 1064 nm, both red-detuned with respect to the dominant $^1S_0 \rightarrow {}^1P_1$ transition in Yb at 399 nm (see Fig. 1). The diamagnetic Yb atoms are intrinsically not affected by the MT, while for Rb the optical potentials cancel to lowest order for equal beam waists and an appropriate power ratio, since the 1064 nm light is red-detuned and the 532 nm light is blue-detuned from the dominant atomic transition in Rb at 780 nm. In this hybrid trap,

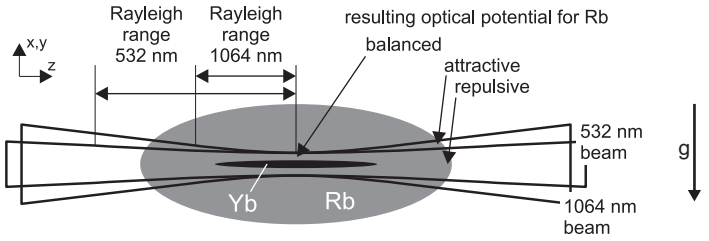

Figure 1. Scheme of the combined trap with the spatial configuration of the atomic clouds and the BIODT laser beams (not to scale).

we have investigated sympathetic cooling of the five isotopes ^{170}Yb, ^{171}Yb, ^{172}Yb, ^{174}Yb and ^{176}Yb through collisions with ^{87}Rb in the $(F = 1, m_F = -1)$ state at temperatures of several 10 μK. A strong dependence of the interspecies collisional cross section on the mass of the ytterbium isotope was observed.

A related trapping scheme which uses only a bichromatic light field for the independent adjustment of the trapping strengths for two species was proposed by Onofrio et al. [27]. Experimentally, a hybrid trap involving a magnetic trapping potential and a single-color light field has recently been used to study the entropy exchange in an ultracold mixture [28].

2. Experimental setup

A typical experimental sequence starts with an Yb magneto-optical trap (MOT) on the broad $^1S_0 \rightarrow {}^1P_1$ transition at 399 nm which is loaded from a Zeeman slower. Up to 2×10^7 Yb atoms are then transferred into a second MOT operating on the narrow $^1S_0 \rightarrow {}^3P_1$ intercombination transition at 556 nm where a density in the range of $10^{11}\,\mathrm{cm}^{-3}$ and a temperature of $\approx 70\ \mu$K are reached. Subsequently, the atoms are loaded into the BIODT by simply turning off the MOT beams. The two light fields of the BIODT have $1/\mathrm{e}^2$-radii of $w_{1064} \approx w_{532} \approx 15\ \mu$m with a residual ellipticity on the order of 10% and typical laser powers of $P_{1064} = 1.0$ W and $P_{532} = 3.4$ W. Stable overlap of the two light fields is achieved by an active stabilization of the relative position. In this configuration, the calculated trap depth for Yb is $U/k_\mathrm{B} \approx -600\ \mu$K and the measured trap frequencies are $\omega_\mathrm{r} \approx 2\pi \times 3.3$ kHz radially and $\omega_\mathrm{z} \approx 2\pi \times 29$ Hz axially. After a time of ≈ 20 s (which is required for the preparation of Rb), the Yb cloud has reached its equilibrium temperature of $\approx 50\,\mu$K through plain evaporation. At this stage, up to 2×10^5 atoms at a density of about $10^{13}\,\mathrm{cm}^{-3}$ are trapped in the BIODT in the case of ^{176}Yb. The lifetime in the BIODT of about 130 s is limited by background gas collisions. For different Yb isotopes, the initial atom number in the optical trap varies by a factor of 2-3 for technical reasons (mainly determined by the specific natural abundance) while the temperature exhibits no significant isotope dependence.

After loading of the BIODT with Yb, a cloud of ultracold Rb is prepared in the same vacuum chamber. In a standard MOT, 10^9 ^{87}Rb atoms at a temperature

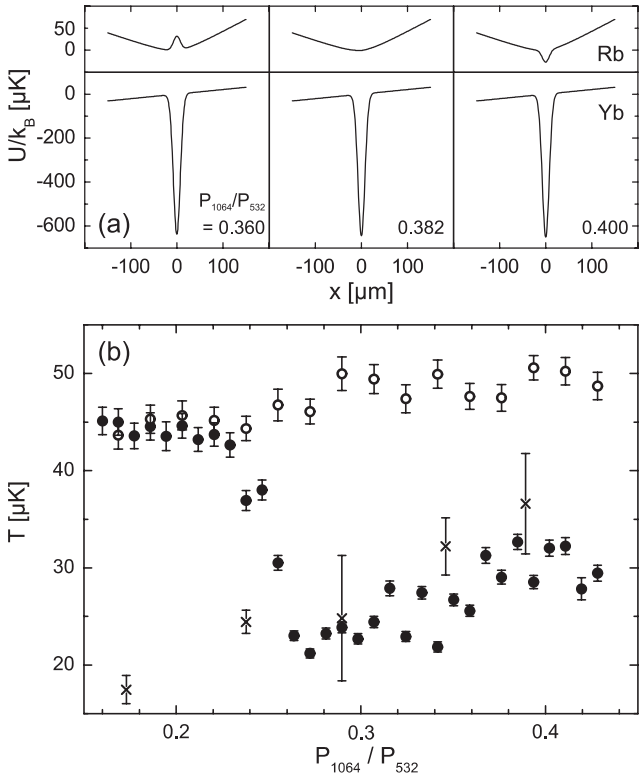

Figure 2. (a) Calculated potentials of the hybrid trap for ^{176}Yb and ^{87}Rb (in the $(F = 1, m_F = -1)$ state) using the experimental parameters in (b) and assuming perfect gaussian laser beam profiles. The subfigures show radial cuts through the center of the combined trap including gravity as a function of the ratio P_{1064}/P_{532} (at $P_{532} = 3.4W$).
(b) Steady state temperatures (after 1 s contact time) in the hybrid trap as a function of the power ratio of the two light fields. Shown are the temperatures of ^{176}Yb with (•) and without (○) Rb present and the Rb temperatures (×).

of several 100 μK are loaded from a Zeeman slower. Care is taken to avoid overlap between the Rb MOT and the optically trapped Yb atoms as this leads to a significant loss of Yb atoms. After loading of the MOT, the Rb atoms are transferred to the clover leaf magnetic trap with measured trap frequencies of $\omega_\mathrm{r} = 2\pi \times 175$ Hz and $\omega_\mathrm{z} = 2\pi \times 13.5$ Hz. In the magnetic trap, we prepare an ensemble of typically 10^7 Rb atoms in the $(F = 1, m_F = -1)$ state at a temperature of $\approx 15\,\mu$K by radio-frequency induced evaporation. The center of the MT is initially located at a distance of 0.7 mm from the BIODT. Due to the diamagnetic ground state of Yb, any magnetic field needed for cooling and trapping of Rb does not interfere with the optically trapped Yb atoms. Subsequently, we move the MT for Rb to the position of the BIODT for Yb within 100ms by applying additional magnetic offset fields. Thus, we can control the beginning and the duration of the contact between the two species. The MT and the BIODT, both have their weak axis aligned along the z-direction to ensure maximum overlap of the two atomic clouds. All atom numbers and temperatures are determined by standard

absorption imaging and time-of-flight techniques.

Figure 2(a) shows radial cuts through the trap center of the calculated total trapping potentials for Yb and Rb for various ratios P_{1064}/P_{532}. The calculation includes all magnetic and optical potentials as well as gravity which is perpendicular to the axis of the BIODT and the magnetic trap. Though Fig. 2(a) is certainly a simplified representation as the trap geometry is reduced to 1-D, it is well-suited for a qualitative discussion of the influence of the power ratio on the hybrid trap. For $P_{1064}/P_{532} = 0.382$, the combined optical potential for Rb vanishes and the radial confinement is determined by the magnetic trapping potential alone. Thus, if optical and magnetic potentials are correctly adjusted, the Yb cloud is trapped in the BIODT at the same spatial position where the Rb cloud is held magnetically. For smaller power ratios, the contribution of the 532 nm laser to the BIODT potential becomes dominant creating a repulsive barrier for Rb in the trap center, and the contact between the two species decreases with increasing barrier height. If the power ratio is too high, an attractive dimple forms for Rb caused by the dominant light shift of the infrared beam at 1064 nm. In this case, contact between Yb and Rb is possible, but the Rb trap is no longer independent from the Yb trap, and forced radio frequency evaporation of Rb is stalled since all magnetic substates are trapped in the attractive optical potential.

3. Results

In the experiment, we observe thermalization of Yb with the colder ^{87}Rb after the two clouds are brought into contact. The time until a steady state temperature is reached ranges from 100 ms to several seconds and depends on the Yb isotope and on the number of ^{87}Rb atoms. In agreement with the discussion above, we found the power ratio of the two BIODT beams to be of crucial importance to reach the lowest Yb temperature as can be seen in Fig. 2(b) where the temperature of an ^{176}Yb cloud is plotted as a function of the power ratio for a fixed contact time. For P_{1064}/P_{532} below a critical value of ≈ 0.25, the Yb temperature is unaffected by the presence of Rb, due to the lack of thermal contact while above this value, Yb thermalizes with Rb. With increasing power ratio, however, the Rb temperature increases due to the influence of the resulting attractive BIODT-potential, leading also to an increase of the steady-state Yb temperature.

The coldest mixtures are obtained at $P_{1064}/P_{532} \approx 1.0\ \mathrm{W}/3.4\ \mathrm{W} \approx 0.29$. The difference to the value of 0.382, which results in light shift compensation for Rb in the model potential, may be attributed to uncontrolled deviations of the experimental optical potential from the calculated one. In addition, cooling of Yb should already be possible for a slightly repulsive potential for Rb if the interspecies collisional cross section is large. To account for this effect in a quantitative way, will require an improved experimental control over the details of the trap geometry. In this context, it is worth noting that the Rb temperature starts to increase already at a power ratio below the critical value. We attribute this to the fact, that the two light fields are not perfectly overlapping and attractive regions in the light field are forming even for low infrared

power. This is partly due to a deviation of the beam shapes from a perfect gaussian shape, but even for perfect gaussian beams, complete overlap of the two light fields is not possible due to the different divergences of the two laser beams (see Fig. 1).

We have studied the thermalization process in the Rb-Yb mixture for the bosonic isotopes ^{170}Yb, ^{172}Yb, ^{174}Yb and ^{176}Yb, which posses all a nuclear spin of $I = 0$, as well as for the fermionic isotope ^{171}Yb with a nuclear spin of $I = 1/2$. After the two ensembles are brought into contact, we record the evolution of the Yb temperature as a function of the contact time. In Fig. 3, a sample curve for ^{176}Yb is shown, which clearly demonstrates sympathetic cooling. We do not observe any loss of Yb atoms during thermalization, as is shown in the inset of Fig. 3. In the case of ^{176}Yb and ^{174}Yb, we measure steady state temperatures close to the Rb temperature, while for the other isotopes the steady-state temperature stays well above the Rb temperature, which may be accounted for by a smaller scattering cross section in combination with additional heating and imperfect spatial overlap of the two atomic clouds. In the case of ^{170}Yb we observe almost no temperature reduction.

During the contact time, the Rb temperature is kept constant by continuously applying a radio frequency of 1.5 MHz to the magnetically trapped Rb atoms. Under this condition, we observe a significant loss of Rb on a timescale of several seconds in the presence of the BIODT light fields. We attribute this loss to an imperfect cancellation of light shifts for Rb which results in an adiabatic compression and heating of the Rb ensemble when the MT is shifted onto the BIODT. In addition, the Rb atoms are heated by photon scattering from the relatively intense BIODT beams. In the presence of a constant radio frequency both heating mechanisms translate into a loss of atoms. This interpretation is supported by another series of experiments, where the radio frequency was turned off during the contact time. In that case, we found the Rb atom number to stay constant but observed a rapid initial increase of the Rb temperature to $\approx 30\,\mu$K within about 130 ms followed by a constant heating of about 1 μK/s (the latter in agreement with the expected heating rate due to photon scattering in the BIODT). Results of both experimental methods have entered into the quantitative analysis below.

From measurements of the thermalization rate at ultracold temperatures as presented in Fig. 3, information about the interspecies cross section σ_{YbRb} can be obtained. For a constant Rb temperature and $N_{\mathrm{Rb}} \gg N_{\mathrm{Yb}}$, the evolution of the Yb temperature can be written as [29]

$$\dot{T}_{\mathrm{Yb}}(t) \;=\; -\gamma_{\mathrm{th}} \cdot \Delta T(t) + \dot{T}_{\mathrm{heat}}\,, \tag{1}$$

with the thermalization rate γ_{th}, and $\Delta T(t) = T_{\mathrm{Yb}}(t) - T_{\mathrm{Rb}}(t)$ the temperature difference between Yb and Rb. The heating rate for Yb, $\dot{T}_{\mathrm{heat}}$, which is taken to be independent of the presence of Rb atoms is measured to be 0.9 μK/s and can be accounted for by photon scattering in the BIODT. Experimentally, we determine the initial cooling rate $\dot{T}_{\mathrm{Yb}}(0)$ and temperature difference $\Delta T(0)$ and thus the initial thermalization rate $\gamma_{\mathrm{th},0} = (\dot{T}_{\mathrm{heat}} - \dot{T}_{\mathrm{Yb}}(0))/\Delta T(0)$ can be expressed in terms of experimentally determined quantities.

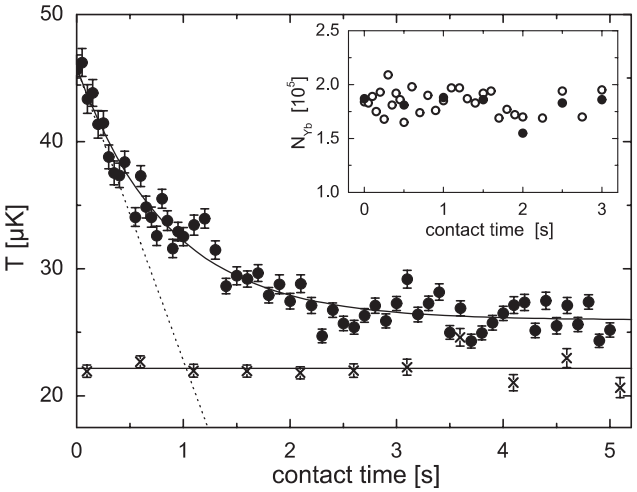

Figure 3. Temperature evolution of ^{176}Yb (•) and ^{87}Rb (×) during thermalization. The solid lines are exponential (Yb) and constant (Rb) fits to the data. The dotted line shows the slope of the exponential fit at $t = 0$ corresponding to the initial cooling rate of Yb. The inset shows the atom numbers for sympathetically cooled Yb (○) and for Yb without Rb present (•).

Assuming as a first approach a temperature-independent scattering cross section σ_{YbRb}, the thermalization rate is on the other hand given by

$$\gamma_{\mathrm{th}} \;=\; \frac{\xi}{\alpha}\,\gamma_{\mathrm{coll}} \;=\; \frac{\xi}{\alpha}\,\sigma_{\mathrm{YbRb}}\,\bar{v}\,n_{\mathrm{YbRb}}\;. \tag{2}$$

Here α is the number of collisions which is required for thermalization if the collisional partners have equal mass [30, 31, 32], ξ is a mass-dependent reduction factor [29], $\bar{v} = \sqrt{(8k_{\mathrm{B}}/\pi)\,(T_{\mathrm{Yb}}/m_{\mathrm{Yb}} + T_{\mathrm{Rb}}/m_{\mathrm{Rb}})}$ the thermal velocity and

$$n_{\mathrm{YbRb}} \;=\; (N_{\mathrm{Yb}}^{-1} + N_{\mathrm{Rb}}^{-1}) \int n_{\mathrm{Yb}}(\mathbf{r}) n_{\mathrm{Rb}}(\mathbf{r}) \mathrm{d}^3\mathbf{r} \;\approx N_{Rb}\, f_{YbRb} \tag{3}$$

the overlap density, where we have introduced an overlap function f_{YbRb}. Introducing the parameter $\beta = (\dot{T}_{\mathrm{heat}} - \dot{T}_{\mathrm{Yb}}(0))\,(\bar{v}_0 N_{\mathrm{Rb}} \Delta T(0))^{-1}$ with the initial thermal velocity $\bar{v}_0$, the scattering cross section can be written as

$$\sigma_{\mathrm{YbRb}} \;=\; \frac{\alpha}{\xi}\,\beta\, f_{YbRb}^{-1}\;. \tag{4}$$

While β is completely determined by experimentally measured quantities and α and ξ can be modeled, the overlap function f_{YbRb} is experimentally difficult to determine precisely as it is strongly influenced by small deviations of the trapping potential from the ideal situation. Due to the composition of the trapping potential of two optical fields and a magnetic field in our experiment, such uncontrolled deviations are experimentally unavoidable, as already mentioned. Thus, precise absolute values of scattering cross sections cannot be determined from our measurements directly. However, it is possible to determine relative cross sections for different Yb isotopes if f_{YbRb} is assumed to be constant. Hence, we define $\beta_{\mathrm{norm}}(^x\mathrm{Yb}^{87}\mathrm{Rb}) = \beta(^x\mathrm{Yb}^{87}\mathrm{Rb})/(5.36 \times 10^{-6}\ \mathrm{m}^{-1})$

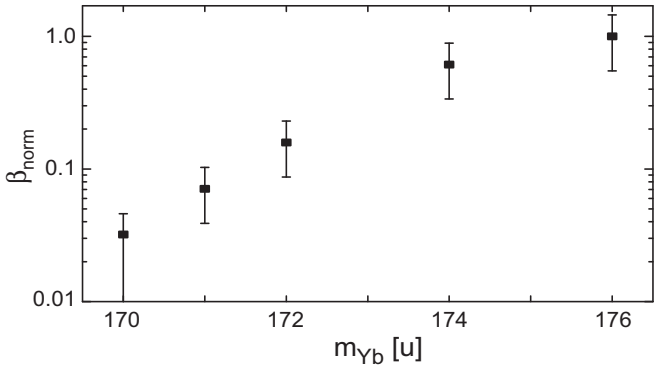

Figure 4. Coefficient $\beta_{\rm norm}$ which is a measure for the relative interspecies scattering cross section between ^{87}Rb and a given Yb isotope at the experimental temperature of $T \approx 50\mu$K.

corresponding to normalizing the interspecies scattering cross section for the isotope ^{x}Yb to the experimentally determined value for ^{176}Yb.

In Fig. 4, the experimentally determined values of $\beta_{\rm norm}$ are shown for all investigated Yb isotopes. The error bars are inferred from the experimental variations of 12 independent measurements of $\beta(^{176}\mathrm{Yb}^{87}\mathrm{Rb})$. These variations are attributed to uncontrolled temporal variations of details of the trap geometry and thus of f_{YbRb}. Within experimental uncertainties, $\beta(^{170}\mathrm{Yb}^{87}\mathrm{Rb})$ is compatible with zero. The observed strong mass dependence of $\beta_{\rm norm}$ is consistent with the scattering properties being determined by details of the molecular potential of ground state YbRb, which in turn are strongly influenced by the mass of the atoms [33]. In recent experimental studies at lower temperatures in the μK regime, that will be reported in detail elsewhere, we have found that for ^{174}Yb the scattering cross section increases significantly for decreasing temperatures and becomes much larger than the one for ^{176}Yb. While this is an obvious violation of the above assumption of a temperature-independent scattering cross section, the values for $\beta_{\rm norm}$ in Fig. 4 are still a good representation of the relative scattering cross sections at the experimental temperature of around $50\,\mu$K as they have been determined using only the initial slope of the thermalization curve (Fig. 3). However, it should be noted that the height of the centrifugal barrier for p-wave-collisions [34], which we have calculated using the C_6-coefficients for Yb and Rb [35, 36, 37], is only around $60\,\mu$K. Thus, a contribution of p-wave collisions to the collisional properties of the Yb-Rb mixture described here may not be excluded.

In order to give at least an estimate of the magnitude of the interspecies cross section in mixtures of Yb and Rb, we have evaluated $\sigma_{^{176}\mathrm{Yb}^{87}\mathrm{Rb}}$ under the assumption of a perfect trap geometry. Under this condition, we calculate a value for the overlap function of $f_{YbRb} \approx 5 \times 10^{10}\,\mathrm{m}^{-3}$ using the experimentally determined temperature and trap parameters of the individual traps. Taking $\alpha \approx 2.7$ as the number of collisions required for thermalization [30, 31, 32] and calculating a reduction factor of $\xi = 0.89$ for the Yb-Rb mixture [29] we obtain $\sigma_{^{176}\mathrm{Yb}^{87}\mathrm{Rb}} = (3.3 \pm 1.5) \times 10^{-16}$ m^2. Here the

error is only statistical and does not include the systematic error due to the overall uncertainties concerning details of the trap geometry which can easily change f_{YbRb} by a factor of 2. Nevertheless, we may still conclude that at a temperature of around 50 μK $\sigma_{^{176}\mathrm{Yb}^{87}\mathrm{Rb}}$ is of a similar magnitude as the s-wave scattering cross section for collisions between ^{87}Rb atoms [36].

4. Conclusion

In conclusion, we have experimentally realized an ultracold mixture of a paramagnetic and a diamagnetic atomic species and thus demonstrated the experimental feasibility to investigate ultracold, conservatively trapped mixtures which combine atomic species that behave very differently in external fields. The trapping geometry in which we have achieved sympathetic cooling of Yb through collisions with Rb may easily be adopted for other combinations of atomic species with similar magnetic properties. It allows for nearly independent manipulation of the trapped species and thus offers a lot of flexibility for experimental studies. In addition, we have determined elastic scattering properties between ^{87}Rb and five different Yb isotopes at $T \approx 50\mu$K and observed a strong dependence on the mass of the Yb isotope. At least for the isotopes ^{176}Yb and ^{174}Yb, the scattering cross sections are large enough for efficient sympathetic cooling with ^{87}Rb as a coolant.

These first results on combined trapping of Rb and Yb open the prospect to realize a novel kind of quantum degenerate mixture. Together with recent experimental [24] and theoretical work [38, 39] on YbRb molecules, the findings presented in this paper will also be valuable for the development of a strategy to create paramagnetic YbRb ground state molecules.

We acknowledge financial support from the Deutsche Forschungsgemeinschaft under the Emmy-Noether program and under SPP 1116. F.B. was supported by a fellowship from the Stiftung der Deutschen Wirtschaft.

[1] Taglieber M, Voigt A C, Aoki T, Hänsch T W and Dieckmann K 2008 *Phys. Rev. Lett.* **100** 010401
[2] Modugno G, Modugno M, Riboli F, Roati G and Inguscio M 2002 *Phys. Rev. Lett.* **89** 190404
[3] Hadzibabic Z, Stan C A, Dieckmann K, Gupta S, Zwierlein M W, Görlitz A and Ketterle W 2002 *Phys. Rev. Lett.* **88** 160401
[4] Roati G, Riboli F, Modugno G and Inguscio M 2002 *Phys. Rev. Lett.* **89** 150403
[5] Silber C, Gunther S, Marzok C, Deh B, Courteille P W and Zimmermann C 2005 *Phys. Rev. Lett.* **95** 170408
[6] Spiegelhalder F M, Trenkwalder A, Naik D, Kerner G, Wille E, Hendl G, Schreck F and Grimm R 2010 *Phys. Rev. A* **81** 043637
[7] Stan C A, Zwierlein M W, Schunck C H, Raupach S M F and Ketterle W 2004 *Phys. Rev. Lett.* **93** 143001
[8] Inouye S, Goldwin J, Olsen M L, Ticknor C, Bohn J L and Jin D S 2004 *Phys. Rev. Lett.* **93** 183201
[9] Thalhammer G, Barontini G, De Sarlo L, Catani J, Minardi F and Inguscio M 2008 *Phys. Rev. Lett.* **100** 210402
[10] Wille E, Spiegelhalder F M, Kerner G, Naik D, Trenkwalder A, Hendl G, Schreck F, Grimm R,

Tiecke T G, Walraven J T M, Kokkelmans S J J M F, Tiesinga E and Julienne P S 2008 *Phys. Rev. Lett.* **100** 053201
[11] Deh B, Marzok C, Zimmermann C and Courteille P W 2008 *Phys. Rev. A* **77** 010701
[12] Pilch K, Lange A D, Prantner A, Kerner G, Ferlaino F, Naegerl H C and Grimm R 2009 *Phys. Rev. A* **79** 042718
[13] Baranov M, Dobrek L, Goral K, Santos L and Lewenstein M 2002 *Physica Scripta* **T102** 74
[14] DeMille D 2002 *Phys. Rev. Lett.* **88** 067901
[15] Micheli A, Brennen G K and Zoller P 2006 *Nature Physics* **2** 341
[16] Kozlov M G and Labzowsky L N 1995 *J. Phys. B* **28** 1933
[17] Hudson J J, Sauer B E, Tarbutt M R and Hinds E A 2002 *Phys. Rev. Lett.* **89** 023003
[18] Sage J M, Sainis S, Bergeman T and DeMille D 2005 *Phys. Rev. Lett.* **94** 203001
[19] Deiglmayr J, Grochola A, Repp M, Moertlbauer K, Glueck C, Lange J, Dulieu O, Wester R and Weidemueller M 2008 *Phys. Rev. Lett.* **101** 133004
[20] Lang F, Straten P V D, Brandstatter B, Thalhammer G, Winkler K, Julienne P S, Grimm R and Hecker Denschlag J 2008 *Nature Physics* **4** 223
[21] Ni K K, Ospelkaus S, de Miranda M H G, Pe'er A, Neyenhuis B, Zirbel J J, Kotochigova S, Julienne P S, Jin D S and Ye J 2008 *Science* **322** 231
[22] Ospelkaus S, Ni K K, Quemener G, Neyenhuis B, Wang D, de Miranda M H G, Bohn J L, Ye J and Jin D S 2010 *Phys. Rev. Lett.* **104** 030402
[23] Knoop S, Ferlaino F, Berninger M, Mark M, Naegerl H C, Grimm R, D'Incao J P and Esry B D 2010 *Phys. Rev. Lett.* **104** 053201
[24] Nemitz N, Baumer F, Münchow F, Tassy S and Görlitz A 2009 *Phys. Rev. A* **79** R061403
[25] Okano M, Hara H, Muramatsu M, Doi K, Uetake S, Takasu Y and Takahashi Y 2010 *Appl. Phys. B* **98** 691
[26] Mewes M, Andrews M, Druten N V, Kurn D, Durfee D and Ketterle W 1996 *Phys. Rev. Lett.* **77** 416
[27] Onofrio R and Presilla C 2002 *Phys. Rev. Lett.* **89** 100401
[28] Catani J, Barontini, Lamporesi, Rabatti F, Thalhammer G, Minardi F, Stringari S and Inguscio M 2009 *Phys. Rev. Lett.* **103** 140401
[29] Mosk A, Kraft S, Mudrich M, Singer K, Wohlleben W, Grimm R and Weidemller M 2001 *Appl. Phys. B* **73** 791
[30] Monroe C, Cornell E, Sackett C A, Myatt C and Wieman C 1993 *Phys. Rev. Lett.* **70** 414
[31] Wu H and Foot C 1996 *J. Phys. B* **29** 321
[32] Arndt M, Dahan M B, Gury-Odelin D, Reynolds M and Dalibard J 1997 *Phys. Rev. Lett.* **79** 625
[33] Ferrari G, Inguscio M, Jastrzebski W, Modugno G, Roati G and Simoni A 2002 *Phys. Rev. Lett.* **89** 053202
[34] Dalibard J 1999 Collisional dynamics of ultra-cold atomic gases *Bose-Einstein Condensation of Atomic Gases. Proceedings of The International School of Physics Enrico Fermi - Course CXL* ed Inguscio M, Stringari S and Wieman C E (IOS Press, Amsterdam) p 321
[35] Kitagawa M, Enomoto K, Kasa K, Takahashi Y, Ciuryło R, Naidon P and Julienne P S 2008 *Phys. Rev. A* **77** 012719
[36] van Kempen E G M, Kokkelmans S J J M F, Heinzen D J and Verhaar B J 2002 *Phys. Rev. Lett.* **88** 093201
[37] Derevianko A 2001 *Phys. Rev. Lett.* **87** 023003
[38] Sorensen L K, Knecht S, Fleig T and Marian C M 2009 *J. Phys. Chem. A* **113** 12607
[39] Meyer E R and Bohn J L 2009 *Phys. Rev. A* **80** 042508